ISBN: 978-3-95450-204-2 ISSN: 2673-5350 doi:10.18429/JACoW-IBIC2019-TUPP037

STUDIES OF THE TIME STRUCTURE OF IONISATION BEAM PROFILE MEASUREMENTS IN THE ISIS EXTRACTED PROTON BEAMLINE

C. C. Wilcox*, W. A. Frank†, A. Pertica, R. E. Williamson, STFC Rutherford Appleton Laboratory, Didcot, Oxfordshire, UK

Abstract

Ionisation Profile Monitors (IPMs) are used at the ISIS neutron and muon source to perform non-destructive transverse beam profile measurements. An in-house particle tracking code, combined with 3D CST modelling of the electric fields within the monitors, has been used to improve understanding of the various error sources within the IPMs, and shows close agreement with profile measurements in the synchrotron.

To allow for detailed benchmarking studies, an IPM has been installed in Extracted Proton Beamline 1 (EPB1), enabling comparison with secondary emission (SEM) grid measurements. However, the IPM measurements taken in EPB1 show increased levels of profile broadening at operational beam intensities, which are not reproduced by SEM measurements or simulation. To investigate these differences, studies of the time structure of measured profiles are being performed.

This paper details the development of new, high-speed multichannel data acquisition electronics, required to perform these studies. Resulting measurements are discussed, along with an analysis of the data's time structure and a comparison with that predicted by the IPM code.

INTRODUCTION

Profile measurements using Ionisation Profile Monitors (IPMs) are inherently affected by both the beam's space charge field and non-uniformities in the monitor's drift field distribution [1]. These effects alter the trajectories of residual gas ions within the monitors, causing them to diverge, broadening the measured profiles. Producing accurate simulation codes to analyse, quantify and correct for this effect is an area of active development at multiple hadron accelerator facilities [2].

A particle tracking code has been developed for ISIS IPMs, to simulate their internal residual ion motion and resulting profile measurements. Previous work and an outline of how this code functions are detailed in [3], though it has since been rewritten in Python. The code is benchmarked against a test IPM, installed in Extracted Proton Beamline 1 (EPB1), to allow for single-pass measurements to be taken and compared with profile data from nearby secondary emission (SEM) grids.

EPB1 transports an 800 MeV pulsed proton beam; each pulse consists of two 100 ns bunches separated by 225 ns. The ISIS synchrotron operates at a repetition rate of 50 Hz, with four of every five pulses extracted to EPB1. The minimum pulse spacing of 20 ms ensures that IPM measurements are unaffected by multi-pass effects. Typical beam intensities are ~3×10^{13} protons per pulse (ppp).

* christopher.wilcox@stfc.ac.uk
† william.frank@stfc.ac.uk

At operating intensities, profiles measured with the EPB1 IPM show unexpectedly high levels of broadening compared with both simulation and synchrotron IPM measurements. To further understand the effects occurring within the monitor, and to provide additional benchmarking data for the IPM code, high-speed data acquisition (DAQ) electronics have been developed to measure the time structure of the measurements taken by this monitor.

IPM CODE DEVELOPMENT

To allow for comparison with the measured time structure, a time-dependant approximation of the beam pulse structure has been added to the IPM simulation code. Two key effects are determined by this: beam-induced generation of residual gas ions and the impact of the beam's space charge field on ion motion within the IPM.

Two separate calculations of the electric field map within the monitor are computed, using CST EM Studio 2018 [4]. One utilises only the drift field electrode and IPM detector biases as electric field sources, while the other also includes the beam space charge field, with the input beam distribution determined by SEM profile monitor measurements. The ion tracking code only takes the space charge component of the electric field into account during the two 100 ns intervals in which a bunch is passing through the IPM. This is achieved by alternating between the two electric field maps at the relevant times during the tracking simulation. Similarly, the code generates residual gas ions continuously during these 100 ns time intervals, with the generated transverse ion distribution also determined by SEM monitor measurements.

DAQ SYSTEM REQUIREMENTS

Risetime and Bandwidth

ISIS IPMs use an array of forty 4800 series Channeltron Electron Multipliers (CEMs), supplied by Photonis [5], to detect residual gas ions. Each CEM is 6 mm wide, providing adequate measurement resolution for typical beam widths in the synchrotron and EPBs (50-120 mm). To estimate the required bandwidth for the DAQ system, the IPM simulation code was used to predict the time structure of the ion current input into the CEMs (Fig. 1a).

All residual gas ions generated in this simulation were H^+ ions (i.e. protons). In addition to being common within beampipe vacuums, the low mass and fast acceleration of H^+ by the drift field means the predicted time structure from this model represents the highest frequency content which the IPM should be expected to measure.

The frequency spectrum of this simulated ion current, obtained from a fast Fourier transform of the simulation output, yields a minimum required bandwidth of 3.5 MHz

ISBN: 978-3-95450-204-2 ISSN: 2673-5350 doi:10.18429/JACoW-IBIC2019-TUPP037

(Fig. 1b). Typical 10-90% rise times of CEMs are 3-5 ns [5], corresponding to a bandwidth of ~70 MHz if the detector is assumed to be a first-order low-pass system, more than sufficient to resolve the expected signal [6].

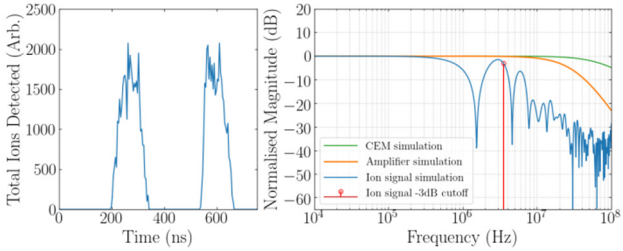

Figure 1: (a) Simulation of H^+ ion arrival at the CEMs in EPB1, (b) Simulated CEM and amplifier frequency responses compared with the ion signal spectrum.

National Instruments (NI) 8-channel, 60 MS/s, 12-bit PXIe-5105 oscilloscope cards were selected for the DAQ system. These have inbuilt 24 MHz anti-aliasing filters which limit the analogue bandwidth to below the Nyquist frequency, while providing sufficient bandwidth for the IPM measurement. Transimpedance amplifiers are required to convert the CEM output current into a measurable voltage. To avoid limiting the measurement bandwidth to below that of the DAQ cards, the 3 dB cut-off frequency of these amplifiers was specified as 30 MHz. In contrast, other IPMs at ISIS use 7 kHz amplifiers which are too slow to resolve the time structure within a beam pulse measurement. Figure 1b shows that the frequency responses of the new amplifier design (simulated with OrCAD PSpice) and a CEM are sufficient to resolve the simulated ion signal spectrum.

Gain and Dynamic Range

Each CEM has an adjustable gain, set by its applied bias voltage, with typical electron multiplication factors between 10^5-10^7. The CEM output current at the beam centre in the EPB1 IPM was measured with a bias voltage of -1.4 kV and a beam intensity of $3\text{x}10^{13}$ ppp, yielding a peak current of 50 µA. From CEM gain calibration data, supplied by Photonis for each detector, this equates to a residual ion current of 100-170 pA, though this estimate may be affected by gain degradation due to ion exposure since the monitor's installation in 2006.

The PXIe-5105 cards have a configurable input ADC range between 0.05-6 Vpp, with 50 Ω input impedance. To match the large dynamic range of the CEM output currents to this input range, the amplifiers were designed with a fixed transimpedance gain of 3000 into a 50 Ω load. This yields an expected dynamic range of 0.03-2.55 V for CEM bias voltages between -1.3 and -1.6 kV, the range over which the gain calibration data is supplied.

AMPLIFIER DESIGN

The transimpedance amplifiers consist of two stages. The first stage, with a voltage gain of 120, uses the Texas Instruments (TI) OPA847, a high gain bandwidth op-amp (3.9 Ghz) with an ultra-low input voltage noise (0.85 nV/√Hz). The second, a unity gain 30 MHz low-pass filter stage, uses the TI OPA656, which provides sufficient bandwidth and slew rate. Each amplifier board mechanically conforms to the Eurocard standard. Custom backplane and interconnection PCBs are used to route the output and control signals to the DAQ system. Each board contains four channels, with each containing the circuitry for both the existing 7 kHz amplifiers and the new 30 MHz amplifiers, including the required relay switching circuits. Figure 2a shows the new amplifier's response to a 10 mV, 100 ns Gaussian pulse, while Fig. 2b shows its frequency response. In each case, there is close agreement between the measurements and PSpice simulations.

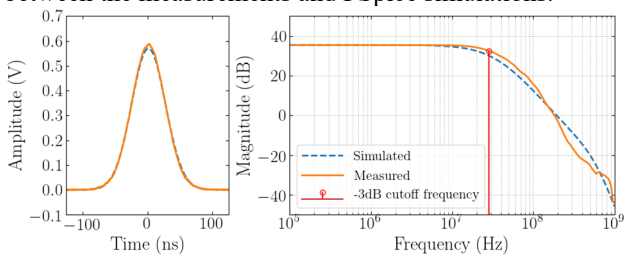

Figure 2: (a) Response of the amplifier to a 100 ns Gaussian pulse and (b) the corresponding frequency response.

DATA ACQUISITION AND SOFTWARE

DAQ Hardware

The ISIS Diagnostics section has standardised on the NI PXI/PXIe platform for DAQ [7]. The DAQ system for the EPB1 IPM consists of: a PXIe-8880 modular PC running LabVIEW RT, a single PXIe-6535 digital I/O card and six 8-channel PXIe-5105 cards, installed in a PXIe-1082 8-slot chassis. A custom timing unit is used to synchronise data acquisition to the EPB1 extraction rate, with each channel simultaneously sampled at 60 MS/s over a configurable time interval, typically 20 µs. If required, the data is then averaged over multiple cycles and sent over the ISIS network to a host PC via TCP/IP.

Software Interface and Gain Calibration

New LabVIEW software has been developed for signal processing, analysis, logging and visualisation of the IPM data on a host PC. The software can be used to process a beam profile measurement by applying the calibration routine developed for ISIS's IPMs [7], used to counteract the variation in gains between individual CEMs. This involves stepping a single 4700 series CEM across the beam aperture using a motorised linear stage. At each stepped position, the motorised CEM is transversely aligned to one of the IPM's fixed CEMs, ensuring that both measure equal ion fluxes. The ratio of output signals from the pair of CEMs, integrated over a configurable time window, is stored and used to scale the outputs from each of the fixed CEMs, normalising their gains.

Calibration is applied in ISIS's synchrotron IPMs by adjusting individual CEM bias voltages [8]. However, all forty CEMs in the EPB1 IPM are biased from a single power supply, so calibration is performed entirely in software. Baseline and background removal is also implemented, along with remote amplifier selection. Control

ISBN: 978-3-95450-204-2 ISSN: 2673-5350 doi:10.18429/JACoW-IBIC2019-TUPP037

of the drift field and CEM bias power supplies is enabled via the ISIS Control System, VISTA VSystem [9].

RESULTS

A source of longitudinal field non-uniformity within ISIS IPMs is the interaction between the drift field and a nearby compensating electrode [3], used in the monitor's calibration procedure, and also to prevent the IPMs applying a net kick to the beam. To simplify the simulations and measurements presented in this section, this electrode was not biased during any of the presented results.

Initial measurements with the new system were taken using the EPB1 IPM, with a nearby SEM grid used to measure inputs for the IPM simulation code. Unless stated otherwise, measurements were taken at beam intensities of ~2.6x10^{13} ppp and with a 15 kV drift field potential.

Profile Measurement Time Structure

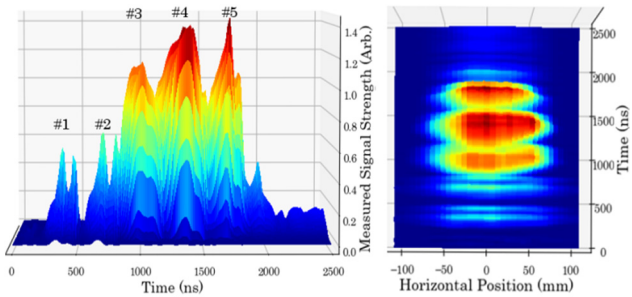

Figure 3: Two views of the time structure measured by the EPB1 IPM, using the new DAQ system.

Figure 3 shows the time structure of a profile measurement, with the time axes set such that t = 0 corresponds to the time at which the first proton bunch enters the IPM. Most of the signal is contained within five distinct peaks (labelled in Fig. 3) spread over a 2 µs period, with varying amplitudes and transverse widths. The first two peaks each contain two maxima, but these are grouped together in this section as their close proximity prevents them being resolved or studied individually.

In addition to the five peaks, two differential signals were measured between 0-100 ns and 325-425 ns, the times at which each bunch passes through the IPM. These are not shown in Fig. 3 but are present in every measurement, even when the IPM's drift field is off, and have fairly uniform magnitudes across the beam aperture. Therefore, it was concluded that these signals are generated by capacitive pickup of the beam's electric field in the CEMs. The monitor's software was modified to include a background removal function, which was used to remove these signals from all results presented in this paper.

Residual Gas Composition

The detection times of the first two peaks in the measurement match those predicted by the IPM code (Fig. 1a). However, these peaks have very small amplitudes, with the vast majority of the signal contained in the latter three peaks, detected around 1-2 µs after the beam passes through the monitor. A possible explanation for this discrepancy can be found by considering the composition of the residual gas. The simulated time structure in Fig. 1a was calculated by assuming that the residual gas within the monitor is comprised entirely of hydrogen. Consequently, all ions in the simulation are H^+, which are accelerated very quickly by the IPM's drift field. However, the residual gas is also likely to contain concentrations of heavier molecules, notably water vapour (which is difficult to remove from vacuum systems) and nitrogen molecules (from any small air leaks). Ionisation products from these would be accelerated at a slower rate, creating a measured signal spread out over a larger time period.

To test the feasibility of this theory, proof–of-concept simulations were performed using the IPM code. Figure 4 shows the simulated time structure of a measurement using a residual ion mix containing H_2O^+, OH^+, H^+, H_2^+, N^+ and N_2^+ ions, with the relative quantities estimated from [10] and mass spectrometer data from the ISIS synchrotron.

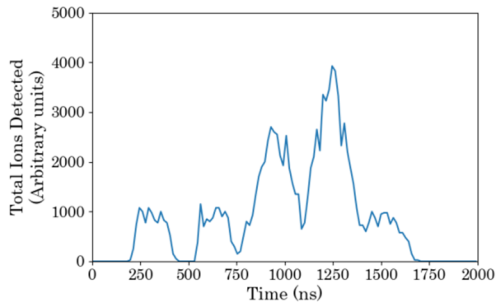

Figure 4: Simulated ion detection times, summed over all CEMs, produced by the estimated mix of residual ions.

Considering this residual ion composition is an estimate, the results show close enough agreement to the measured data to justify further investigation, with a multi-peak structure spread out over a comparable time period. Mass spectrometer measurements of the residual gas composition in EPB1 will be taken to provide an accurate ion composition for the IPM simulation code. Adding ionisation cross section data and a fully time-dependant space charge field, varying with the longitudinal structure of each bunch, will also be considered for the code.

Varying Drift Field Strengths

It is important to establish whether each component of the time structure is generated by beam-induced residual gas ions, so that the correct way to process the measurement can be determined. For instance, if all parts of the signal are generated by residual ions, then they all contain valid beam profile data in some form. However, if there is a secondary source introducing noise into part of the signal, this can be mitigated by specifying a targeted integration window to exclude it from the measurement.

To determine if each peak in the time structure is generated by heavier residual ion species, the IPM's drift field was swept from 3-30 kV, to study the effect on the measured time structure. Figure 5 contains a subsection of the results, showing measurements taken with a single CEM located at the centre of the aperture.

ISBN: 978-3-95450-204-2 ISSN: 2673-5350 doi:10.18429/JACoW-IBIC2019-TUPP037

As the drift field strength increases, the detection times of all signal components are reduced, and the data becomes more clearly resolved into the multiple distinct peaks. An exception is the second peak, which is partially absorbed by the third, larger peak at values of 15 kV and above. At lower drift fields, the separation between the maxima within each of the first two peaks increases, suggesting these are in fact separate overlapping peaks, likely generated by H^+ and H_2^+ ions.

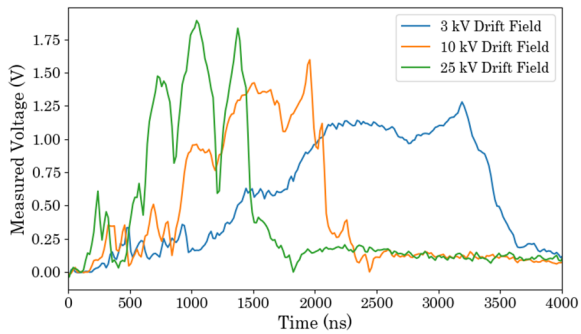

Figure 5: The effect of varying the drift field bias on the measured time structure.

The drift field accelerates residual gas ions towards the CEMs via the Lorentz force, with acceleration given by:

$$a = \frac{qE_y}{m} \tag{2}$$

where: q and m are the charge and mass of the ions respectively and E_y is the electric field component in the direction of acceleration. By assuming each ion has no initial velocity, this can be related to the time taken for ions to reach the CEMs, t, using the equations of motion:

$$t = \left(\frac{2l}{a}\right)^{1/2} \tag{3}$$

where l is the distance travelled to reach the CEMs. As E_y and a are proportional, if the drift field is increased, the time taken for ions to be detected should decrease proportionally to the inverse square root of the field amplitude.

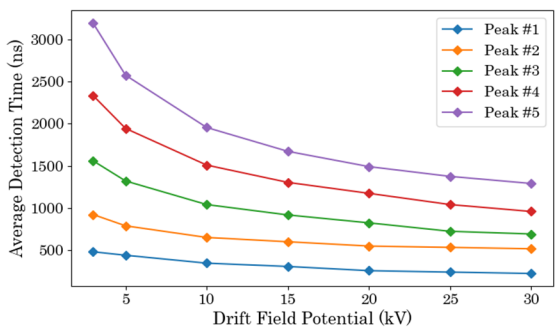

Figure 6: The effect of varying drift field strength on the average detection times of each peak.

This trend can be seen clearly in Fig. 6, in which the average detection time of each peak decreases as the drift field potential is increased. This decrease is slightly less pronounced for the first and second peaks due to the constant acceleration supplied by the beam's space charge field, which affects the faster moving ions over a larger proportion of their travel time and is not considered in Eq. (2). The trends shown in Figs. 5 and 6 suggest that all peaks within the signal are generated by residual ions, and therefore can each be expected to contain valid profile data, generated by the beam.

Profile Data Analysis

There is significant variation between the beam profiles contained in each specific peak (Table 1). Profiles contained in the third and fourth peaks match closely, while the profile contained in the fifth peak is similar, though around 20% narrower. The 95% widths calculated from the first two peaks are significantly broader compared with the rest of the signal. However, these have smaller amplitudes, resulting in a lower signal to noise ratio, which could explain this. The software removal of capacitive pickup in the CEMs also overlaps with these peaks, which may have an effect. Full width at half maximum (FWHM) values, which are less affected by noise, show a closer agreement between the initial and final peaks.

Table 1: Beam Profiles Calculated from Each Peak

Peak Number	95% Width [mm]	FWHM [mm]
1	127.3 ± 6	74.2 ± 6
2	125.4 ± 6	70.2 ± 6
3	98.7 ± 6	85.5 ± 6
4	97.1 ± 6	86.5 ± 6
5	83.4 ± 6	69.2 ± 6
Total Signal	*104.3* ± 6	*74.5* ± 6

The differences in individual peak widths may be due to their varying levels of exposure to the beam's space charge field. For example, the ions which generate the final peak are created entirely by the second bunch passing through the IPM, and hence will be less exposed to the broadening effect of the space charge field compared with those generated by the first bunch. Similarly, the first two peaks are made up of fast travelling ions, which may also be exposed to a reduced proportion of the space charge field. Further studies are required for clear conclusions to be made, along with accurate modelling of the time-varying space charge field in the IPM simulation.

SUMMARY AND FUTURE WORK

A high-speed multichannel amplifier system has been designed, characterised and installed on the test IPM in ISIS EPB1. Multiple distinct peaks can be seen in the time structure of beam profile measurements taken with the system. The studies presented in this paper indicate that this time structure is caused by a range of ion species generated from the EPB1 residual gas composition. All components of the measured signal appear to contain valid beam profile data, with variations between the widths of each peak potentially caused by varying levels of exposure to the beam's space charge field.

To allow for more accurate comparisons with simulation, the residual gas composition in EPB1 will be measured. In addition, the IPM simulation code will be developed to include a fully time dependant space charge field component, which varies over time to reflect the longitudinal structure of each proton bunch within the beam.

ISBN: 978-3-95450-204-2 ISSN: 2673-5350 doi:10.18429/JACoW-IBIC2019-TUPP037

REFERENCES

[1] D. Vilsmeier, "Space-Charge Distortion of Transverse Profiles Measured by Electron-Based Ionization Profile Monitors and Correction Methods", *Physical Review Accelerators and Beams,* vol. 22, no. 5, p. 052801, 2019.

[2] M. Sapinski *et al.*, "Ionization Profile Monitor Simulations – Status and Future Plans", in *Proc. IBIC2016,* Barcelona, Spain, Sep. 2016, paper TUPG71.

[3] C. C. Wilcox, B. Jones, A. Pertica, and R. E. Williamson, "An Investigation into the Behaviour of Residual Gas Ionisation Profile Monitors in the ISIS Extracted Beamline", in *Proc. IBIC2016,* Barcelona, Spain, Sep. 2016. doi:10.18429/JACoW-IBIC2016-WEPG68

[4] CST, http://cst.com

[5] *Channeltron Electron Multiplier Handbook for Mass Spectrometry Applications,* Burle Electro-Optics Inc., USA, 2001. https://www.triumf.ca/sites/default/files/ChannelBookBurle.pdf

[6] T. J. Sobering, "*Bandwidth and Risetime",* Kansas State University, Manhattan, USA, May 1999.

[7] S. J. Payne *et al.* "Beam Diagnostics at ISIS", in *Proc. HB'08*, Nashville, TN, USA, Aug. 2008, paper WGF10.

[8] S. A. Whitehead, P. G. Barnes, G. M. Cross, S. J. Payne and A. Pertica, "Multi-Channeltron Based Profile Monitor at the ISIS Proton Synchrotron,", in *Proc. BIW10*, Santa Fe, NM, USA, Apr. 2010, paper TUPSM007.

[9] B. Mannix and T. Gray, "Vista Controls VSystem at the ISIS Pulsed Neutron Facility," presented at *ICALEPCS'07*, Knoxville, TN, USA, Oct. 2007.

[10] J. H. Miller, "Differential Cross Sections for Ionization of Water Vapour by High-Velocity Bare Ions and Electrons", *Journal of Chemical Physics*, vol.86, no. 157, pp. 157-162, 1987.